Kinetics of Cellulase Saccharification of Corn Stover after Pretreatment by Lignin Peroxidase and H_2O_2

Zhi C. Zhang,[a,*] Jin H. Li,[b] and Feng Wang [b]

The kinetics of cellulase saccharification of corn stover (CS) after pretreatment by lignin peroxidase (LiP) and H_2O_2 was modeled in this work. The Impeded Michaelis model was applied in fitting all experimental data. The model gave the initial activity and accessibility of the enzyme on the substrate ($K_{obs,0}$) and the gradual loss of enzyme activity (K_i). The maximum Y_{trs} (55.56%) was obtained at pH 4.7, 48.6 °C, a 1.5% cellulase, and 12.4:1 water-to-material ratio. The binary quadratic model provide a good fit of the data on Y_{trs} and of the model parameters $K_{obs,0}$ and K_i. The results showed that Y_{trs} was positively correlated with $K_{obs,0}$ and negatively correlated with K_i. This study laid a foundation for improving the cellulase saccharification efficiency of lignocellulosic biomass after pretreatment by H_2O_2 and LiP.

Keywords: Kinetics; Heterogeneous system; Enzyme hydrolysis; Impeded Michaelis model; Binary quadratic model

Contact information: a: Institute of Agro-production Processing Engineering, Jiangsu University, 306 Xuefu, Zhenjiang, Jiangsu 212013, P. R. China; b: School of Food and Biological Engineering, Jiangsu University, 306 Xuefu, Zhenjiang, Jiangsu 212013, P. R. China;
** Corresponding author: zhangzhicai@ujs.edu.cn*

INTRODUCTION

Lignocellulosic biomass represents a variety of biomass sources, including agricultural waste, where lignocelluloses can be utilized as raw materials and converted into valuable chemicals, food products, and/or bio-energy (Baeyens *et al*. 2015). The conversion of cellulose from lignocelluloses into bioenergy has attracted a great deal of interest among researchers (Kang *et al*. 2014). However, only a minimal amount of lignocellulose is typically utilized. As such, a great quantity of lignocellulose has been wastefully discarded, resulting in environmental pollution and a serious waste of natural resources. Lignin inhibits the degradation of cellulose and hemicellulose by preventing contact with the cellulase and hemicellulase (Shi *et al*. 2008; Bellido *et al*. 2014; Wang *et al*. 2015). The crystal structure reduces access to the surface area between cellulase and cellulose, and between hemicellulose and hemicellulase. Therefore, the aim of the pretreatment is to degrade the lignin and to improve enzymatic saccharification efficiency. The H_2O_2 oxidative degradation is a particularly promising pre-treatment method (Ramadoss and Muthukumar 2015; Zhang *et al*. 2015; Cao *et al*. 2016; Qing *et al*. 2016). The catalysts used in H_2O_2 oxidative degradation of lignin include alkali (Cao *et al*. 2016), inorganic salt (Ramadoss and Muthukumar 2015; Qing *et al*. 2016), and enzymes (Zhang *et al*. 2015). However, the use of alkali and inorganic salt as catalysts results in environmental pollution. The potential advantages of enzymatic-H_2O_2 oxidative degradation of lignin include cost-effectiveness, speed, convenience, safety, high yield of total reducing sugar (Y_{trs}), low environmental impact, and the lack of a need for special

equipment. However, the hydrolysis solution of this method contains high amounts of lignin degradation products. These degradation products may affect the next step in the saccharification of cellulose catalyzed by cellulase.

A kinetic model that completely describes the enzymatic hydrolysis process is essential for reactor design. The Michaelis–Menten model for enzyme kinetics is well suited for application in homogeneous systems. However, many bio-catalytic reactions take place in heterogeneous systems where the effects of mass-transfer and reaction occur, such as accessibility and reactivity of enzymes on insoluble substrates, and enzyme deactivation (Xu and Ding 2007; Bansal *et al*. 2009). Previous studies have proposed alternative models to simulate enzymatic reactions in a heterogeneous system, such as the jammed Michaelis model, the fractal Michaelis model, and the model of the shrinking particle theory (Movagharnejad and Sohrabi 2003; Xu and Ding 2007; Bansal *et al*. 2009). These models have the following disadvantages: (i) the models consist of complicated ordinary differential equations that must be solved; (ii) the models contain many parameters that cannot be effectively determined; and (iii) some parameters are arbitrarily selected rather than research supported (Ye and Berson 2011). To overcome the above-mentioned disadvantages of these models, the Impeded Michaelis model has been developed by modifying the Michaelis-Menten model with a time-dependent decay coefficient of impeded enzyme reaction (Yang and Fang 2015a, 2015b). However, this model cannot directly show the correlation between the yield of total reducing sugar (Y_{trs}) and the initial activity and accessibility of the enzyme on the substrate ($K_{obs,0}$) or the gradual loss of enzyme activity (K_i) in a heterogeneous system.

In the authors' previous study, *Aspergillus oryzae* CGMCC5992 was isolated from the sludge of the Yudai River at Jiangsu University, and was able to remove chemical oxygen demand (COD) from vinasse (Zhang *et al*. 2013). When gallic acid is used as the substrate, *Aspergillus oryzae* CGMCC5992 can synthesize lignin peroxidase (LiP), and laccase (Guo *et al*. 2013). Proteomic analysis has shown that the strain secretes LiP in the presence of corn stover (CS) (Guan *et al*. 2015). These enzymes play key roles in the degradation of lignin and aromatic compounds. Furthermore, the authors have developed a method to degrade lignin in CS by combining solid state fermentation and enzymatic hydrolysis, and have found that *A. oryzae* grows well on H_2O_2-pretreated CS. This method has a higher synthesis of LiP, a greater disintegration of lignin (Zhang *et al*. 2014), a reduced treatment time of 10 days rather than 50 days, and an increased efficiency of lignin degradation of 80% compared to the 57.8% efficiency of solid-state fermentation (Zhang *et al*. 2014). However, it has two major drawbacks of requiring a large production location and having a long fermentation cycle. Recently, a combination of liquid-state fermentation and enzymatic hydrolysis has been applied in the pretreatment of CS, and the Y_{trs} reaches a maximum of 46.28% (Zhang *et al*. 2015). In the present study, the authors aimed to further explore the kinetics of enzymatic hydrolysis of cellulose from the CS pre-treated by LiP and assess the effects of various factors on the enzymatic hydrolysis kinetics. Moreover, the authors investigated the correlations between Y_{trs} and $K_{obs,0}$ and between Y_{trs} and K_i in a heterogeneous system and clarified the enzymatic saccharification law of cellulose in the presence of the degradation products of lignin. This study will help to optimize hydrolysis conditions to lay the foundation for next step in ethanol fermentation, which might include using CS as a raw material.

EXPERIMENTAL

Materials

The CS was obtained from a local farm (Jurong, China) and ground to less than 0.25-mm. The content of hemicellulose, cellulose, and lignin of the ground CS consisted of 26.24%, 32.12%, and 15.42%, respectively. A commercial *Trichoderma reesei* cellulase was purchased from Guangzhou Global Green Tech. Ltd. (Guangzhou, China). The activities of carboxymethyl-cellulase (CMCase), filter paper enzyme (FPase), β-glucosidase, and hemicellulase were 5.97×10^4 U/mL, 821 FPU/mL, 10.1 U/mL, and 284 U/mL, respectively. All chemicals used were of analytic grade and purchased from East China chemical and glass- Instruments Co. Ltd. (Zhenjiang, China).

Microorganism

The *A. oryzae* CGMCC5992 applied in the study was isolated from the sludge of the Yudai River at Jiangsu University and stored in the China General Microbiological Culture Collection Center. The strain in all of the experiments was cultured on PDA slants at 28 °C for 4 days, then stored in refrigerator at 4 °C and transferred every 2 months.

LiP preparation

The crude LiP solution was prepared according to the method described by Zhang *et al*. (2015) with minor modifications. A total of 1×10^6 spores from the *A. oryzae* slant were inoculated aseptically into a 250-mL Erlenmeyer, loading 100 mL potato dextrose medium and then incubated in a rotary incubator shaker at 35 °C, 125 rpm for 24 h. This culture broth was used as seed in the LiP fermentation. Subsequently, 10 mL of seed culture was aseptically inoculated into a 250-mL Erlenmeyer flask containing 100 mL of minimal medium (pH 6.8 to 7.0). The minimal medium consisted of: 30 g/L CS powder, 2.5 g/L glycerol, 2.5 g/L maltose, 15 g/L yeast extraction, 4.5 g/L $(NH_4)_2SO_4$, 0.4 g/L $FeSO_4 \cdot 7H_2O$, 0.4 g/L $CuSO_4 \cdot 5H_2O$, 1 g/L $MnSO_4 \cdot H_2O$, 0.6 g/L $MgSO_4 \cdot 7H_2O$, 0.1 g/L VB_{12}, and 0.004 g/L glycine. After inoculation, the flask was incubated at 35 °C in a rotary incubator shaker (125 rpm) for 72 h. Then, the incubation broth was centrifuged, and the supernatant was examined to determine the LiP activity. The LiP activity was adjusted to 500 U/L, and the supernatant was used as an enzyme in the lignin hydrolysis.

Oxidative degradation of CS by H_2O_2 using A. oryzae CGMCC 5992 broth as catalyst

Next, 20 g CS was mixed with 250 mL H_2O in a 500-mL three-neck round-bottom flask, and the mixture was pretreated at 110 °C for 10 min and then cooled to 35 °C. Subsequently, 75 mL enzyme solution (the above-described LiP-containing supernatant) was added to the flask, and the mixture solution was stirred at 100 rpm and preheated to 35 °C in the water bath. Then, 100 mL H_2O_2 (1.5%) was added to the mixture at a flow rate of 0.5 mL/min. After 8 h of hydrolysis, the mixture was filtered, and the filtered residue was dried to a constant weight and used as raw material in the cellulase saccharification reaction. The lignin content of the filtered residue (the pretreated CS) was 9.8%.

Cellulose saccharification in CS after enzymatic catalysis by A. oryzae CGMCC 5992 broth

All saccharification tests of pretreated CS cellulose were conducted in 250-mL Erlenmeyer flasks. First, 10 g CS pretreated with H_2O_2 and LiP was added into 100 mL of 0.1 mol/L acetate buffer containing 1% cellulase (pH 4.5). After being fully mixed, the

initial concentration of reducing sugar was denoted as C_0. The saccharification reaction was conducted at 50 °C in a shaking bath (120 rpm) for 12 h. Then, 1-mL samples were collected at 4 h, 8 h, 12 h, 24 h, and 48 h. Each sample was immediately cooled in an ice bath to room temperature to terminate the reaction. The reducing sugar concentration in each flask was denoted as C_1. The Y_{trs} was calculated according the following equation,

$$Y_{trs}\ (\%) = C \times V / G \times 100 \quad (1)$$

where Y_{trs} is the yield of total reducing sugar, V is the volume of reaction solution (mL), G is the weight of total dry substrate (g), and C_1 and C_0 are the reducing sugar concentrations (g/mL) at 0 h and t h of reaction.

Methods

One-factor-at-a-time test

Various factors, including pH, water to materials ratio, temperature, and enzyme concentration, were assessed by the one-factor-at-a-time method. The pH values of the acetate buffer were 2, 3, 4, 5, 6, and 7, respectively. Water to materials ratios were 8:1, 10:1, 12:1, 14:1, and 16:1, respectively. Temperature was set at 35 °C, 40 °C, 45 °C, 50 °C, 55 °C, and 60 °C, respectively. The enzyme concentration was 0.5%, 0.75%, 1%, 1.25%, 1.5%, and 2%, respectively.

Response surface design

The effects of reaction temperature, pH of acetate buffer, water to materials ratio, and enzyme concentration on Y_{trs} were evaluated *via* the Box–Behnken Design (BBD) modification of the response surface design (Amini *et al*. 2009a, 2009b; Cerino-Córdova *et al*. 2011, 2012; Dávila-Guzmana *et al*. 2012). A four-factor and three-level response surface analysis was designed using Y_{trs}, the initial observed rate constant ($K_{obs,0}$), and the coefficient of the ineffective enzyme during the hydrolysis reaction (K_i) as response variables. The reaction pH of the acetate buffer, temperature, water-to-material ratio, and cellulase concentration were used as independent variables. Table 1 shows the levels of the variables that were identified from the results of the one-factor-at-a-time experiments.

Table 1. Factors and Levels of Box-Behnken Design of Response Surface*

Level	pH	Temperature	Enzyme Concentration	Water/Materials Ratio
	A	B	C	D
-1	4	40	0.5	8
0	5	50	1.0	12
1	6	60	1.5	16

*: The units of temperature and enzyme concentration were °C and %.

Analysis

The LiP activity of the broth was spectrophotometrically (Shanghai Analytical Instrument Co., Ltd., Shanghai, China) measured according to the method described by Mitchell and Lonsane (1993). The reaction solution consisted of 1.5 mL of 10 mM veratryl alcohol, 50 μL enzyme sample, and 0.25 M sodium tartrate buffer (pH 2.5). The reaction

was initiated by adding H_2O_2 (5 mM). One unit (U) of LiP activity was defined as the amount of enzyme required to oxidize 1 μmol veratryl alcohol to veratryl aldehyde in 1 min at 30 °C. The total lignin content (acid-soluble lignin + acid-insoluble lignin) of substrates and raw materials was determined as recommended by Sluiter *et al*. (2008). The reducing sugar concentration in the hydrolysis solution was identified according to the 3,5-dinitrosalicylic acid method (Miller 1959).

All tests were repeated at least three times, and the results were presented as means due to their negligible standard errors. All data were fitted using Microsoft Excel (Microsoft, Redmond City, America) and SPSS 17.0 software (IBM, Ammonst City, USA). The analysis of Box–Behnken Design (BBD) was performed with the Design-Expert version (8.0.4). All the regression equation and the analysis of variance (ANOVA) were performed using SPSS 17.0 software.

Impeded Michaelis kinetic model

The enzymatic saccharification of CS pretreated with H_2O_2 and LiP was conducted in a heterogeneous system, in which many factors affect the reaction kinetics. These factors include product inhibition, mass-transfer resistance, interaction between enzyme and the inert, nonreactive site of lignocellulosic biomass, and enzyme inhibition (Gan *et al*. 2003). Based on the Michaelis–Menten model with minor modifications, the impeded kinetic model in a heterogeneous system constructed by Yang *et al*. (2015a, 2015b) was applied to fit all of the test data.

Michaelis–Menten model believes that the enzymatic reaction process is divided into two step including that the substrate (S) combined with enzyme (E) forms the enzyme-substrate complex (ES) and that ES is converted into E and product (P).

According to impeded Michaelis kinetic model, the efficiency dependent upon the pretreatment on the substrate, the initial accessibility of cellulase to the cellulose of pretreated CS, and the activity of cellulase on the cellulose ($K_{obs,0}$) = $k_2(E_0)$ / K_m, the correlation between the yield of total reducing sugar (Y_{trs}), reaction time (t) and $K_{obs,0}$ was as follows,

$$\frac{dY_{trs}}{dt} = K_{obs,0} \times \frac{1}{(1 + \alpha t)} (1 - Y_{trs}) \quad (2)$$

where E_0 is the initial enzyme concentration, k_2 is the rate constants from enzyme-substrate complex to product, K_m is the Michaelis constant, and α is a constant. The coefficient of the time-dependent inactive enzyme (K_i) can be calculated according to the constant α and the following equation,

$$K_i = \frac{2\alpha}{1 + \alpha t} \quad (3)$$

where inactive enzyme results from the combined effects of product inhibition, the action of enzyme on the inert and nonreactive site of lignocellulose biomass, and the mass-transfer resistance for enzymes. Equation 2 can be solved to give:

$$-\ln(1 - Y_{trs}) = \frac{K_{obs,0} t}{1 + \alpha t} \quad (4)$$

Equation 4 then can be rearranged as,

$$\frac{t}{-\ln(1-Y_{trs})} = \frac{1}{K_{obs,0}} + \frac{\alpha}{K_{obs,0}} t \quad (5)$$

where Eq. 5 was applied to fit the experimental results by plotting t / (−ln(1 – Y_{trs})) *versus* t. The coefficient of t term and the constant term are α / $K_{obs,0}$ and 1 / $K_{obs,0}$, respectively. The value for K_i was calculated according to Eq. 3, and the predicted Y_{trs} ($Y_{trs,\,pred}$) was calculated under optimum condition according to the equation below.

$$Y_{trs,pred} = 1 - e^{(-\frac{K_{obs,0}t}{1+\alpha t})} \quad (6)$$

RESULTS AND DISCUSSION

In the enzymatic degradation of solid cellulose, the action of cellulase in the mobile components of insoluble cellulosic substrates produces chemical and physical changes, resulting in an increased release of the residual lignin or lignin monomer in the residual solid phase of pretreated CS (Balat and Balat 2008). Because the enzymatic saccharification of cellulose is a rather slow process, these actions and the feedback inhibition of the products are negligible in the initial reaction stage.

One-factor-at-a-time Method

All Y_{trs} determined at various time in the one-factor-at-a-time are shown in Table 2. Table 3 shows $K_{obs,0}$ and K_i obtained from the regression equation and the ANOVA of the data. All p values were less than 0.01 and R^2 was close to adj-R^2 in Table 3, which implied that all fitted equations were statistically significant (p<0.05) and all data were reliable.

Effect of water to materials ratio

The addition of water may have three effects on the system. Firstly, it will tend to favor enzyme diffusion from the solution to the reaction interface, and the product diffusion from the reaction interface to the solution. Secondly, addition of water affects the microenvironment of the enzyme, which can affect catalytic activity and susceptibility to denaturation (Liu *et al*. 2010; Salum *et al*. 2010; Liu *et al*. 2011). Thirdly, water protects the cellulase from combining residual lignin and degrading products, which further affects the reaction velocity. However, if the water-to-material ratio is too high, it will reduce the concentrations of enzyme and substrate, which will decrease the reaction rate. Similarly, high water-to-material ratio leads to lower ethanol concentration, increasing the cost of subsequent ethanol-water distillation, and the volume of reactors. Therefore, the optimal water-to-material ratio must provide enzymatic saccharification and require low cost to concentrate the final product. The authors studied the effect of the water-to-material ratio on the saccharification kinetics of cellulose, as shown in Table 2. Table 3 reveals the variation tendency of parameters $K_{obs,\,0}$, and K_i from the kinetic equation (5) with an increase of water to materials ratio. Tables 2 and 3 shows that (1) Y_{trs} at 12 h of reaction and $K_{obs,\,0}$ gradually increased from 39.60% to 50.42%, and from 0.2762 h^{-1} to 0.3537 h^{-1}, respectively, when the water to materials ratio increased from 8:1 to 10:1, and that they gradually decreased with further increase of the water to materials ratio; (2) K_i presented a U-shaped curve when the water to materials ratio was changed within the tested range; (3) the minimum K_i (0.1231 h^{-1}) was obtained at a water to materials ratio of 12:1. Because $K_{obs,0}$ = k_2[E_0] / K_m and [E_0] was the initial cellulase concentration and a constant in the

experiment, an increase of $K_{obs,0}$ hinted at an increase of k_2 or decrease of K_m. The K_m value represents the affinity of the reaction between the enzyme and substrate. When K_m was smaller, the affinity was greater and *vice versa*. Because K_i was the coefficient of the ineffective enzyme during the hydrolysis reaction, a lower K_i indicated that there was less ineffective enzyme and more effective enzyme. Therefore, it was deduced that the water to materials ratio increased Y_{trs} by adjusting the affinity between the enzyme and substrate, which led to an increased amount of effective enzyme. Under the condition of a lower water to materials ratio, diffusion was limited, $K_{obs,0}$ decreased, K_i increased, and Y_{trs} decreased. Under the condition of a higher water to materials ratio, the concentrations of cellulase and substrate decreased, as did Y_{trs}.

Table 2. Yield of Total Reducing Sugar (Y_{trs}) in One-Factor-at-a-Time (%)

	Hydrolysis-time (h)					
	0	4	8	12	24	48
Water:Materials Ratio						
8:1	14.0404± 0.9650	16.6804± 0.5101	40.0532± 0.1744	39.5956± 0. 1273	38.8916± 1.173	38.6988± 0.6331
10:1	16.9900± 0.2917	21.2036± 0.9788	48.9764± 0. 7791	50.4196± 0. 2189	48.5322± 0.1715	48.3956± 0.3349
12:1	16.8388± 0.1977	14.5156± 0.9877	44.7172± 0.9318	45.5621± 0.7993	45.9844± 0.9631	47.0404± 1.0010
14:1	9.3942± 0.1892	9.3947± 0.1770	27.1172± 0.9656	28.5076± 0.8653	28.7524± 0.7793	29.3876± 0.7455
16:1	6.1384± 0.2031	9.0948± 0.2644	19.4436± 0.7263	24.4948± 0.1912	24.8292± 0.6549	25.0578± 0.8679
pH						
2	10.0452± 0.2372	13.5652± 0.1110	37.6426± 0.1486	38.0116± 0.3741	39.4548± 0.1641	39.7364± 0.4221
3	10.6612± 0.2458	15.3604± 0.4840	40.1061± 0.1797	40.4404± 0.4195	41.8132± 0.5417	42.5172± 0.7321
4	14.9204± 0.6723	16.9092± 0.8554	44.1364± 0.5730	46.2132± 0.9045	47.7092± 0.8620	49.0468± 0.8185
5	18.2292± 0.7431	21.2036± 0.7064	45.9316± 0.5992	46.1780± 0.6444	47.1284± 0.3158	44.3476± 0.3682
6	15.4484± 0.3357	17.7540± 0.2823	42.6932± 0.9519	43.0918± 0.6843	46.9524± 0.7802	47.9732± 0.2541
7	11.2596± 0.1828	23.2980± 0.4035	41.0036± 0.3601	41.8660± 0.7701	43.2740± 0.2660	42.7108± 0.1965
Temperature (°C)						
35	10.5556± 0.2493	12.3508± 0.0953	23.1748± 0.1139	24.5652± 0.2675	24.8468± 0.1486	25.4452± 0.1950
40	9.1652± 0.2238	11.4118± 0.3598	26.7313± 0.1542	27.9444± 0.2872	28.2436± 0.4626	30.0916± 0.2654
45	11.4356± 0.4137	14.5156± 0.5701	34.3332± 0.4457	36.0404± 0.8595	37.3252± 0.8087	38.3461± 0.4488
50	13.0372± 0.4802	14.5156± 0.4881	43.6436± 0.4673	45.5268± 0.6353	46.1076± 0.3090	47.0052± 0.5286
55	13.9876± 0.2114	19.7604± 0.1907	40.0532± 0.7448	42.1652± 0. 6694	42.8516± 0.7120	41.8132± 0.4924
60	9.8516± 0.1170	13.4772± 0.2855	32.1674± 0.2815	36.4161± 0.8162	37.9764± 0.8581	39.6836± 0.7918

Enzyme Concentration (%)						
0.5	7.0004± 0.1653	12.0692± 0.4978	31.9748± 0.5796	32.8372± 0.9350	33.2068± 0.3544	34.9188± 0.3215
0.75	13.0196± 0.2187	15.8004± 0.7945	37.2548± 0.5837	39.5076± 0.6677	39.7188± 0.4033	40.1236± 0.6628
1	12.9668± 0.5709	17.226± 0.6901	44.6468± 0.9326	45.0164± 0.6993	46.7412± 0.9692	46.9348± 06988
1.25	12.9492± 0.6420	16.8036± 0.2681	47.4804± 0.3445	47.8155± 0.8489	48.1668± 0.3544	48.8884± 0.6405
1.5	13.1604± 0.2825	17.226± 0.3807	48.0084± 0.6721	48.3780± 0.1398	48.9060± 0.8126	49.5572± 1.0239
1.75	13.0027± 0.1608	16.3284± 0.1291	47.4987± 0.2657	48.1316± 0.4033	49.3988± 1.0171	51.3172± 0.3237
2.0	13.8292± 0.1354	17.3316± 0.1830	49.5572± 0.3325	50.6484± 0.9692	50.842± 0.2572	51.7396± 1.7521

Table 3. Results of Regression Analysis in One-Factor-at-a-Time Experiment

	R^2	Adj. R^2	$K_{obs,0}$ (h^{-1})	K_i (h^{-1})	p value*
Water:Materials Ratio					
8:1	0.9758	0.9691	0.2762	0.1443	0.000
10:1	0.9726	0.9659	0.3537	0.1431	0.000
12:1	0.9267	0.9071	0.1650	0.1231	0.0021
14:1	0.9508	0.9386	0.1065	0.1286	0.001
16:1	0.9695	0.9626	0.0932	0.1303	0.000
pH					
2	0.9529	0.9407	0.1597	0.1295	0.001
3	0.9593	0.9492	0.1810	0.1307	0.001
4	0.9487	0.9356	0.1839	0.1249	0.001
5	0.9777	0.9721	0.4523	0.1496	0.000
6	0.9619	0.9516	0.1860	0.1264	0.001
7	0.9914	0.9883	0.3939	0.1485	0.000
Temperature (°C)					
35	0.9907	0.9873	0.1626	0.1441	0.000
40	0.9749	0.9672	0.1214	0.1322	0.000
45	0.9694	0.9617	0.1621	0.1316	0.000

50	0.9263	0.9088	0.1625	0.1225	0.002
55	0.9825	0.9772	0.3166	0.1449	0.000
60	0.9573	0.9468	0.1298	0.1230	0.001
Enzyme Concentration (%)					
0.5	0.9604	0.9506	0.1310	0.1287	0.001
0.75	0.9708	0.9627	0.1996	0.1356	0.000
1	0.9572	0.9463	0.2097	0.1310	0.001
1.25	0.9447	0.9299	0.2054	0.1286	0.001
1.5	0.9457	0.9312	0.2107	0.1288	0.001
1.75	0.9309	0.9126	0.1755	0.1210	0.002
2	0.9363	0.9207	0.2064	0.1260	0.002

*: *p* value is Prob > F

Effect of pH

The shape of the pH effect curve on the Y_{trs}, $K_{obs,0}$, and K_i of a hydrolysis reaction was determined by the pH. The pH could change the structure of enzymes and the charge quantities on the binding and catalysis sites of enzymes, thus affecting the reaction velocity. In the present study, the authors compared the pH effect of reaction resolution on Y_{trs}, $K_{obs,0}$, and K_i of the cellulose saccharification reaction of pretreated CS. The Y_{trs} in Table 2 and $K_{obs,0}$ in Table 3 had a maximum, respectively, and K_i presented a wavy-value with pH change within the tested range, as shown in Table 3. The maximum response of Y_{trs} and $K_{obs,0}$ occurred between a pH of 4.0 to 5.0. The results showed that pH increased Y_{trs} by increasing the affinity of the enzyme and the substrate, or the reaction velocity from the enzyme-substrate complex to the product when pH was increased from 2.0 to 4.0. The authors' result was different from the results of the cellulase hydrolysis of Douglas fir treated with a wet explosion pretreatment using CCD, where 5.5 is the optimal pH for the maximum Y_{trs} (Biswas *et al*. 2015a,b). This discrepancy could have been explained by differences in the substrates and the sources and properties of the cellulase. The primary driving force for enzyme action is binding cellulase *via* their surface hydrophobic properties, which can be affected by suspension pH through surface functional groups (Lan *et al*. 2012). The wavelike K_i curve shows that the pH effect on the combination of the inhibitor (lignin) and the site in the enzyme was unsynchronized with the pH change.

Effect of temperature

An increase in the reaction temperature might have increased the saccharification reaction velocity, though this occurred only over a strictly limited temperature range. The reaction velocity is initially increased as an increasing temperature certainly increases the mobility of molecules, but also increase the kinetic constant of the reaction (Arrhenius equation). However, the kinetic energy of the enzymes exceeded the energy barrier for

breaking the weak hydrogen and hydrophobic bonds. At a higher temperature, denaturation predominated, accompanied by a loss of catalytic activity.

To explore the optimal temperature of saccharification, the authors performed the saccharification reaction at a series of temperatures, (35 °C, 40 °C, 45 °C, 50 °C, 55 °C and 60 °C) and investigated the effect of reaction temperature on Y_{trs}, $K_{obs,0}$, and K_i , as shown in Table 2 and Table 3.

Tables 2 and 3 show the variation tendency for the Y_{trs}, $K_{obs,0}$ and K_i. The maximum Y_{trs} (45.53%) at 12 h of reaction was obtained at 50 °C (Table 2), while the maximum $K_{obs,0}$ (0.3166 h^{-1}) was obtained at 55 °C (Table 3). The K_i was gradually decreased from 0.1441 h^{-1} to 0.1225 h^{-1} when the temperature increased from 35 °C to 50 °C (Table 3). The K_i then increased from 0.1225 h^{-1} to 0.1449 h^{-1} when the temperature was further increased from 50 °C to 55 °C. Based on these results, the authors deduced that when the temperature was lower than 50 °C, the increase in temperature increased the affinity between the substrate and enzyme, and facilitated the conversion of the enzyme-substrate complex into product, which resulted in a decreased concentration of ineffective enzyme, increased concentration of effective enzyme, and an increased Y_{trs}. When the temperature was between 50 °C and 55 °C, the increase in temperature enhanced the affinity between the substrate and the enzyme, and facilitated the conversion of the enzyme-substrate complex into product. However, the amount of ineffective enzyme also increased.

Effect of enzyme concentration

Enzyme concentration was found to be a key factor in controlling the speed of CS saccharification. In general, higher enzyme concentration led to an increased Y_{trs}. Tables 2 and 3 show the effect of cellulase concentration on Y_{trs}, $K_{obs,0}$, and K_i. Table 3 summarizes the results of the ANOVA analysis. All p values were less than 0.01 and R^2 was close to the adj-R^2 in Table 3, which suggested that these equations provided a good fitting degree. From Table 2 and Table 3, it was clear that when the enzyme concentration increased from 0.5% to 1.5%, Y_{trs} at 12 h of reaction gradually increased from 32.84% to 48.38%, and $K_{obs,0}$ increased from 0.1310 h^{-1} to 0.2107 h^{-1}. However, K_i remained stable within a range of enzyme concentrations. This finding could have been explained by the substrate absorption. Many studies have reported that solid substrate can absorb some enzymes (Vallander and Eriksson 1987; Lee *et al*. 1994; Rosgaard *et al*. 2007). Unsurprisingly, the Y_{trs} increased with enzyme concentration. When the enzyme concentration in the reaction mixture was very low, the substrate (CS) adsorbed fewer enzymes, and the Y_{trs} and $K_{obs,0}$ were positively correlated with enzyme concentration. Therefore, when the enzyme concentration was less than 1.5%, Y_{trs} and $K_{obs,0}$ rapidly increased with enzyme concentration. However, after substrate adsorption reached the saturation state, the excessive enzymes in the solution could not be absorbed, and the Y_{trs} and $K_{obs,0}$ were slowly increased when the enzyme concentration increased from 1% to 2%. This finding could have been explained by substrate limitation.

Optimization of LiP Synthesis Conditions Using RSM

Based on the results of the one-factor-at-a-time method, the water to materials ratio, pH, reaction temperature, and cellulase concentration were selected as the most influential factors. The authors further investigated the effect of their interactions on the Y_{trs}, $K_{obs,0}$, and K_i of the saccharification kinetics of cellulose in CS using BBD with four factors, three levels, and three response values (a total of 29 experiments, as shown in Table 4). Three levels were coded as -1, 0, and +1 (Dávila-Guzmana *et al*. 2012). The second-order

polynomial equation to fit the experimental results and identify the relevant model terms was based on Eq. 7 as follows,

$$Y = \beta_0 + \Sigma\beta_i X_i + \Sigma\beta_{ij} X_i X_j + \Sigma\beta_{ii}(X_i)^2 \quad (7)$$

where Y is the predicted response, β_0 is the constant, β_i is the linear coefficient, β_{ij} is the interaction coefficient, β_{ii} is the quadratic coefficient, and X_i and X_j are the coded independent variables (Cerino-Córdova 2012).

Table 4. Box-Behnken Design of Response Surface Method and the Run Results

Run	A: pH	B: Temperature (°C)	C: Enzyme Concentration (%)	D: Water/ Materials Ratio	Response Value		
					$K_{obs,0}$ (h^{-1})	K_i (h^{-1})	Y_{trs}* (%)
1	5	50	1.0	12	0.1827	0.1221	49.3099
2	5	60	1.5	12	0.2290	0.1268	50.5982
3	6	50	1.0	16	0.2499	0.1311	47.7805
4	5	60	1.0	16	0.1111	0.1043	41.6416
5	6	50	0.5	12	0.2272	0.1474	27.7886
6	6	40	1.0	12	0.2101	0.1460	27.3029
7	5	50	1.0	12	0.2210	0.1213	56.9131
8	4	50	1.5	12	0.2589	0.1257	57.5890
9	5	50	1.5	16	0.1464	0.1226	38.9611
10	4	40	1.0	12	0.1835	0.1387	32.9842
11	5	40	1.0	8	0.0897	0.1291	23.3411
12	4	50	1.0	16	0.0870	0.1166	28.3782
13	5	50	0.5	8	0.0682	0.1291	17.9626
14	5	50	0.5	16	0.1011	0.1256	26.8576
15	5	60	1.0	8	0.1400	0.1340	27.4930
16	4	50	0.5	12	0.0797	0.1129	28.6968
17	5	60	0.5	12	0.1545	0.1310	34.9694
18	6	60	1.0	12	0.1286	0.1370	24.6206
19	6	50	1.5	12	0.1756	0.1378	31.5902
20	4	50	1.0	8	0.0760	0.1282	19.8211
21	4	60	1.0	12	0.1070	0.1365	22.1725
22	5	50	1.0	12	0.1613	0.1228	44.4734
23	6	50	1.0	8	0.1467	0.1409	23.8762
24	5	50	1.0	12	0.1752	0.1260	45.5506
25	5	40	1.0	16	0.3427	0.1449	43.0214
26	5	40	1.5	12	0.2446	0.1315	49.7957
27	5	40	0.5	12	0.1178	0.1242	32.0549
28	5	50	1.0	12	0.2420	0.1322	47.2613
29	5	50	1.5	8	0.1988	0.1322	41.6592

*****: Y_{trs} was the yield of total reducing sugar at 12 h of reaction

Tables 5 and 6 exhibit the authors' test data conducted with the independent variable t and the three dependent variables Y_{trs}, $K_{obs,0}$, and K_i of each run in the response surface designs, respectively. After plotting the t / $-\ln(1 - Y_{trs})$ *vs.* t of the experimental data in 29 runs, it was fitted with Eq. 5, the corresponding regression equation, and the R^2, adj-R^2, and p values are shown in Table 6. All p values were less than 0.01 and R^2 was close to adj-R^2 in Table 6, which suggested that the 29 fitted equations were highly significant.

Table 5. Yield of Total Reducing Sugar (Y_{trs}) at Various Hydrolysis Time of Each Run of Response Surface (%)

Run	Hydrolysis-time(h)					
	0	4	8	12	24	48
1	13.5200± 0.3200	16.4096± 0.2972	47.6868± 0.8513	49.3092± 0.9460	50.6048± 0.4309	51.5064± 0.2369
2	18.9184± 0.1968	21.2868± 0.6706	48.8664± 1.0423	50.5924± 0.8838	53.2848± 0.3591	54.8856± 0.5208
3	19.0096± 0.1892	24.3536± 0.2587	46.0064± 0.5973	47.7848± 0.6196	51.1568± 1.0208	53.4148± 0.3921
4	19.5616± 0.4015	19.8476± 0.3926	24.1824± 0.4015	41.6416± 0.3926	48.8506± 0.4762	50.0052± 0.5811
5	14.0352± 0.7093	16.3884± 0.8693	26.7788± 0.1492	27.7864± 0.3836	28.4436± 0.5406	29.2452± 0.2033
6	14.2996± 0.4726	16.1976± 0.6002	26.5032± 0.2828	27.3088± 0.3189	28.3168± 0.3698	29.2674± 0.3964
7	18.9184± 0.3680	19.3152± 0.5840	55.7028± 1.3442	56.9112± 1.0583	58.4264± 1.0549	59.0848± 0.3698
8	18.9184± 0.1899	22.3156± 0.2598	56.4972± 0.5990	57.5896± 1.8118	59.0848± 0.1109	60.3618± 0.3228
9	16.2572± 0.3880	16.4208± 0.4516	34.1264± 0.5755	38.9612± 1.2878	42.5098± 0.1306	44.3256± 0.2932
10	10.0696± 0.2294	14.6924± 0.6769	31.2532± 0.6685	32.9816± 0.2850	33.7872± 0.6745	34.2516± 0.0978
11	7.0032± 0.0978	9.5146± 0.1381	19.3548± 0.1231	23.3412± 0.3361	24.2848± 0.2480	25.2516± 0.5686
12	7.8244± 0.5099	10.0408± 0.0573	25.3088± 0.1669	28.3724± 0.5194	31.7012± 0.5615	33.1651± 0.6243
13	5.5508± 0.4628	7.6284± 0.0872	15.7392± 0.0989	17.9656± 0.3140	18.2308± 0.4205	20.0884± 0.3682
14	7.8244± 0.1472	10.6344± 1342	26.6332± 0.1300	26.8576± 0.2183	28.6032± 0.3867	30.8216± 0.1968
15	14.2572± 0.4753	15.1376± 0.6327	26.9272± 0.2820	27.4926± 0.2981	30.0236± 0.3757	32.2608± 0.3992
16	5.1612± 0.3893	9.6668± 0.6439	23.5664± 0.1231	28.6983± 0.1972	31.63248± 0.4108	33.3006± 0.4318
17	6.2424± 0.1246	14.2784± 0.1048	32.8968± 0.6752	34.9644± 0.6819	36.2364± 0.7137	37.4872± 0.5231
18	11.7768± 0.1710	12.9428± 0.2247	22.7608± 0.2418	24.6264± 0.2762	25.5068± 0.3109	27.3624± 0.4971
19	13.2396± 0.1246	15.7948± 0.1048	30.3092± 0.6752	31.5024± 0.6919	32.4624± 0.7136	34.3472± 0.5231
20	5.6144± 0.1011	8.0316± 0.2246	18.5276± 0.2418	19.8212± 0.4971	21.3176± 0.1821	22.4932± 0.1710
21	10.5124± 0.2207	9.8242± 0.1869	20.2244± 0;2418	22.1748± 0.1987	22.6312± 0.2415	23.5456± 0.2719
22	16.8024± 0.1761	14.5228± 0.2247	42.6188± 0.4891	44.4744± 0.5219	45.9948± 0.5831	46.4376± 0.5311
23	12.9508± 0.1249	14.0324± 0.2218	22.0792± 0.3721	23.8716± 0.4321	25.5676± 0.4973	26.5952± 0.4733
24	16.8236± 0.1869	14.5016± 0.1971	44.6352± 0.2418	45.5506± 0.5421	45.9796± 0.4869	46.0332± 0.4597
25	23.6192± 0.1710	25.8168± 0.1982	39.5892± 0.7210	43.0214± 0.4532	43.8308± 0.4531	44.9362± 0.8932

26	14.7772± 0.1019	20.4176± 0.3768	47.2628± 0.5231	49.7968± 0.7135	51.0264± 0..8967	51.6756± 0.8700
27	3.7508± 0.061	12.8156± 0.2184	28.8464± 0.4921	32.0588± 0.3219	33.7448± 0.4327	36.0254± 0.4710
28	18.3288± 0.1782	20.6084± 0.3782	46.3724± 0.5537	47.2628± 0.4740	50.1754± 0.6773	50.5712± 0.4547
29	14.4772± 0.1906	16.8524± 0.2899	40.5328± 0.5002	41.6572± 0.6247	43.3488± 0.6703	43.9112± 0.3867

Table 6. Regression Analysis of Each Run of RSM *: *p* value is Prob > F

Run	R^2	Adi-R^2	$K_{obs,0}$ (h^{-1})	K_i (h^{-1})	p value.*
1	0.9276	0.9093	0.1827	0.1221	0.002
2	0.9624	0.9521	0.2290	0.1268	0.001
3	0.9812	0.9767	0.2499	0.1311	0.000
4	0.9228	0.9020	0.1111	0.1043	0.002
5	0.9957	0.9939	0.2272	0.1474	0.000
6	0.9945	0.9936	0.2101	0.1460	0.000
7	0.9209	0.9001	0.2210	0.1213	0.002
8	0.9460	0.9323	0.2589	0.1257	0.001
9	0.9667	0.9581	0.1464	0.1226	0.000
10	0.9815	0.9768	0.1835	0.1387	0.000
11	0.9752	0.9698	0.0897	0.1291	0.000
12	0.9463	0.9327	0.0870	0.1166	0.001
13	0.9787	0.9732	0.0682	0.1291	0.000
14	0.9653	0.9562	0.1011	0.1256	0.000
15	0.9880	0.9856	0.1400	0.1341	0.000
16	0.9384	0.9236	0.0797	0.1129	0.001
17	0.9713	0.9639	0.1545	0.1310	0.000
18	0.9902	0.9870	0.1286	0.1370	0.000
19	0.9872	0.9836	0.1756	0.1378	0.000
20	0.9721	0.9668	0.0760	0.1282	0.000
21	0.9833	0.9795	0.1070	0.1365	0.000
22	0.9305	0.9122	0.1613	0.1228	0.002
23	0.9949	0.9925	0.1467	0.1409	0.000
24	0.9288	0.9119	0.1752	0.1260	0.002
25	0.9943	0.9929	0.3427	0.1449	0.000
26	0.9641	0.9554	0.2446	0.1315	0.000
27	0.9661	0.9586	0.1178	0.1242	0.000
28	0.9693	0.9615	0.2420	0.1322	0.000
29	0.9668	0.9587	0.1988	0.1322	0.000

Table 7. ANOVA Analysis for Quadratic Response Surface Model Fitting

Item	$K_{obs,0}$			K_i			Y_{trs}		
	Co-efficient	F Value	p-value*	Co-efficient	F Value	p-value	Co-efficient	F Value	p-value
Model		3.81	<0.0067		3.67	0.0103		3.58	0.0116
Intercept	16.75			0.12			152.86		
A	2.88	4.43	0.0497	0.0068	13.76	0.0023	-0.56	0.064	0.8034
B	-2.65	3.74	0.0690	-0.0037	4.14	0.0613	-0.58	0.071	0.7942
C	4.21	9.42	0.0066	0.0005	0.90	0.7689	8.49	14.59	0.0017
D	2.66	3.75	0.0685	-0.0040	4.87	0.0444	6.04	7.57	0.0156
AB	-0.13	0.01	0.9582	-0.0017	0.28	0.6064	2.03	0.29	0.6014
AC	-5.77	5.90	0.0258	-0.0056	3.10	0.1002	-6.27	2.72	0.1212
AD	2.31	0.94	0.3444	-0.0004	0.020	0.8899	3.84	1.02	0.3301
BC	-1.31	0.30	0.5892	-0.0029	0.83	0.3776	-0.53	0.019	0.8915
BD	-0.75	8.81	0.0082	-0.011	12.87	0.0030	-1.38	0.13	0.7215
CD	-2.31	0.81	0.3809	-0.0015	0.23	0.6377	-2.90	0.58	0.4586
A^2	-	-	-	-0.0068	7.52	0.0159	-11.15	13.94	0.0022
B^2	-	-	-	0.0050	4.01	0.0651	-6.47	4.7	0.0478
C^2	-	-	-	-0.00034	0.019	0.8293	-2.91	0.95	0.3465
D^2	-	-	-	-0.0007	0.080	0.7813	-10.12	11.50	0.0044
Lack of fit value	-	2.26	0.224	-	2.43	0.2037	-	2.92	0.1570
R^2	-	-	0.9176	-	-	0.9578	-	-	0.9468
Adj-R^2	-	-	0.9030	-	-	0.9312	-	-	0.9329

*: *p* value is Prob > F

The ANOVA testing was useful in that it could be used to determine the "goodness of fit" of a quadratic model. Table 7 summarizes the ANOVA results. Three quadratic models' F values of Y_{trs}, $K_{obs,0}$, and K_i were 3.58, 3.81, and 3.67, respectively, which indicated that three developed quadratic models were significant ($p < 0.05$). There was only a 1.16%, <0.67%, and 1.03% chance for Y_{trs}, $K_{obs,0}$, and K_i, respectively, that a model F value could occur due to chance. Because the three models showed insignificant "lack of

fit F values", which were 2.92, 2.26, and 2.43, respectively, three response values of Y_{trs}, $K_{obs,0}$, and K_i were sufficiently explained by three regression equations.

The goodness of fit of the three models was also confirmed by the R^2 values of the three regression models. The R^2 values of Y_{trs}, $K_{obs,0}$, and K_i were 0.9486, 0.9176, and 0.9578, respectively, which were higher than the highest reported R^2 value of 0.80 in a model with good fit (Govarthanan *et al*. 2015). These results indicated that the predictability of the three models was relatively more reliable, and that the three response values of Y_{trs}, $K_{obs,0}$, and K_i were sufficiently explained by the three regression equations. Their adjusted R^2 was 0.9329, 0.9030, and 0.9312, which was close to their R^2 values, and indicated a good adjustment of the theoretical response values to the experimental data by the developed model. The three regression relationships were given in three equations as follows,

$$Y_{trs} = 48.70 - 0.56 \times A - 0.58 \times B + 8.49 \times C + 6.04 \times D + 2.03 \times AB - 6.27 \times AC + 3.84 \times A \times D - 0.53 \times B \times C - 1.38 \times B \times D - 2.90 \times C \times D - 11.15 \times A^2 - 6.47 \times B^2 - 2.91 \times C^2 - 10.12 \times D^2 \quad (7)$$

$$K_{obs,0} = 0.17 + 0.029 \times A - 0.027 \times B + 0.042 \times C + 0.027 \times D - 0.0013 \times A \times B - 0.058 \times A \times C + 0.023 \times A \times D - 0.013 \times B \times C - 0.070 \times B \times D - 0.021 \times C \times D \quad (8)$$

$$K_i = 0.12 - 0.011 \times B \times D + (6.797 \times A - 3.727 \times B + 0.5490 \times C - 4.045 \times D - 1.673 \times A \times B - 5.585 \times A \times C + 0.4473 \times A \times D - 2.892 \times B \times C - 1.528 \times C \times D + 6.832 \times A^2 + 4.989 \times B^2 + 0.3437 \times C^2 - 0.7052 \times D^2) \times 10^{-3} \quad (9)$$

where *A* is pH, *B* is temperature (°C), *C* is enzyme concentration (%), and *D* is water to materials ratio.

The *p* values of "Prob > F" of the model term were less than 0.0500, which indicated that the terms were significant. Terms C, D, A^2, B^2, and D^2 were significant in the Y_{trs} model. In the $K_{obs,0}$ model, terms A, C, AC, and BD were signifcant, and terms A, D, BD, and A^2 were significant terms in the K_i model. Therefore, the Y_{trs} model contained two linear terms (C, D), three quadratic terms (A, B, and D), and one block term; the $K_{obs,0}$ model contained two linear terms (A, C), two interaction terms (AC and BD), and one block term; the K_i model consisted of two linear terms (A, D), one interaction term (BD), one quadratic term (A^2), and one block term.

The contour plots were constructed to study the interaction among the various factors and to optimize each factor for optimal production (Beg *et al*. 2003; Tanyildizi *et al*. 2005). Figure 1 illustrates 2D contour plots with the effects of temperature, water to materials ratio, pH, and, cellulose concentration on $K_{obs,0}$ and the effects of temperature and water to materials ratio on K_i. Figure 1a shows that when the temperature was increased from 40 °C to 60 °C, and the water to materials ratio decreased from 16:1 to 8:1, $K_{obs.0}$ decreased from its maximum to its minimum. Figure 1b demonstrates that when the pH cellulase concentration increased within the tested range, $K_{obs,0}$ rapidly increased. Figure 1c shows the effects of temperature and water to materials ratio on K_i. When the temperature increased from 40 °C to 50 °C and the water to materials ratio increased from 8:1 to 16:1, the K_i gradually decreased, whereas when the temperature was further increased from 55 °C to 60 °C, the K_i increased.

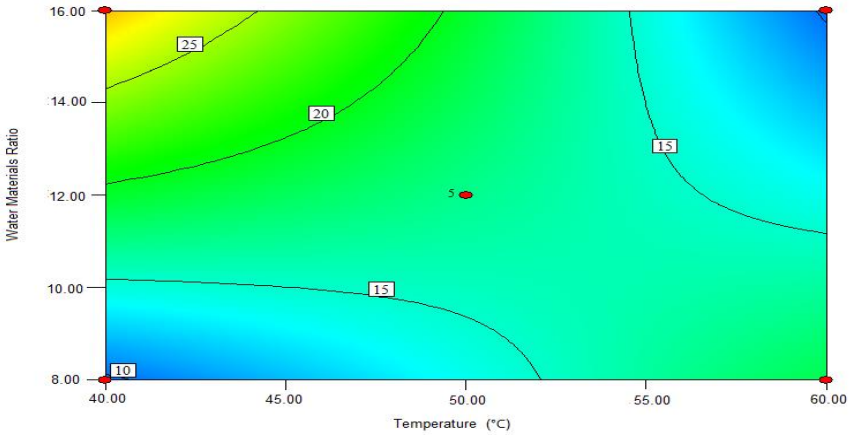

(a)

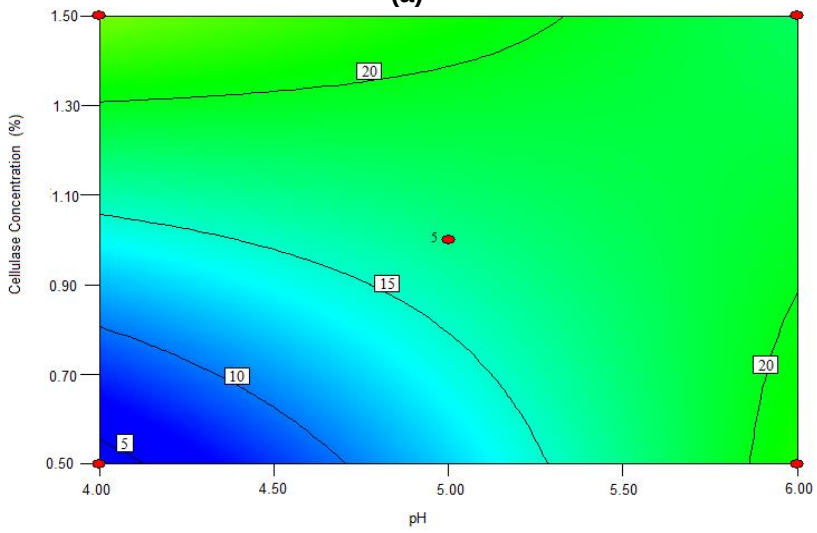

(b)

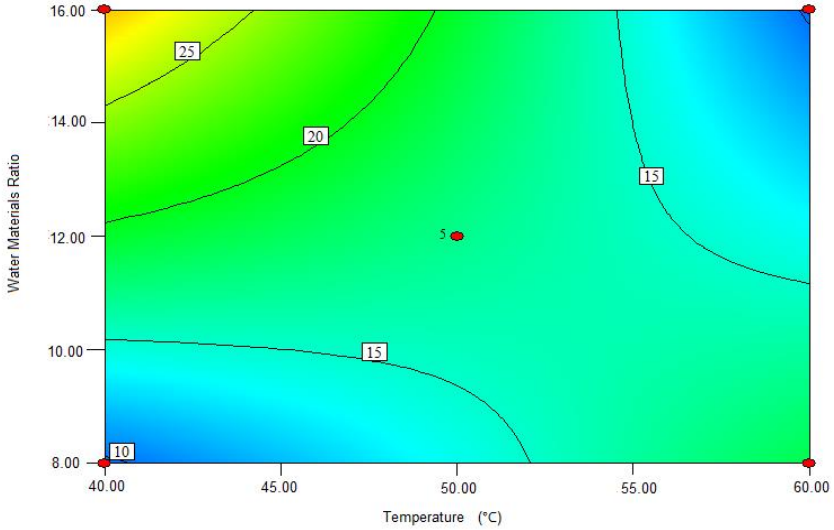

(c)

Fig. 1. The contour plots of the response surface methods; (a) Effects of temperature and water to materials ratio on $K_{obs,0}$; (b) Effects of pH and cellulase on $K_{obs,0}$; and (c) Effects of temperature and water to materials ratio on K_i

To verify the effects of the four variables on Y_{trs}, $K_{obs,0}$, and K_i, the authors further analyzed the perturbation plots as shown in Fig. 2. Figure 2a shows that the effect curves of pH, temperature, and water to materials ratio on the Y_{trs} resulted in an inverted-U-shaped curve, and that the effect curve of cellulase concentration on Y_{trs} resembled a line. The optimal condition for the maximum Y_{trs} was a pH of 4.7, a temperature of 48.6 °C, a cellulase concentration of 1.5%, and a water to materials ratio of 12.4. Under such conditions, the maximum $Y_{trs,pred}$ was 55.56%. Figure 2b shows that the effect curves of the four variables on the $K_{obs,0}$ were close to straight lines. The cellulase concentration was positively correlated with $K_{obs,0}$, whereas other variables were negatively correlated with $K_{obs,0}$. The optimal conditions predicted for $K_{obs,0}$ were a pH of 6.0, a temperature of 40 °C, a cellulase concentration of 0.53%, and a water to materials ratio of 16:1. Under such conditions, the maximum $K_{obs,0}$ was 0.3656 h^{-1}. Figure 2c shows that the effect curves of pH and temperature on K_i presented a U-shaped curve, and the effect curves of cellulase concentration and water to materials ratio on K_i were close to a line. The optimal condition for the minimum K_i was a pH of 4.0, a temperature of 60 °C, a cellulase concentration of 0.55%, and water to materials ratio of 16:1. Under such conditions, the minimum predicted K_i was 0.1100 h^{-1}.

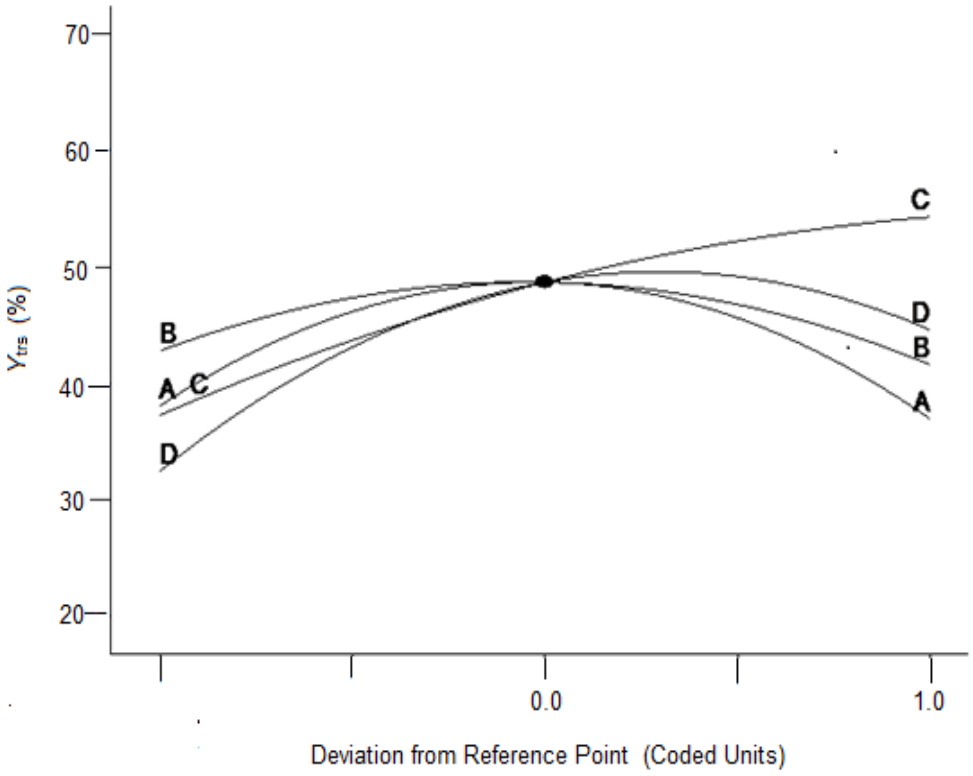

(a)

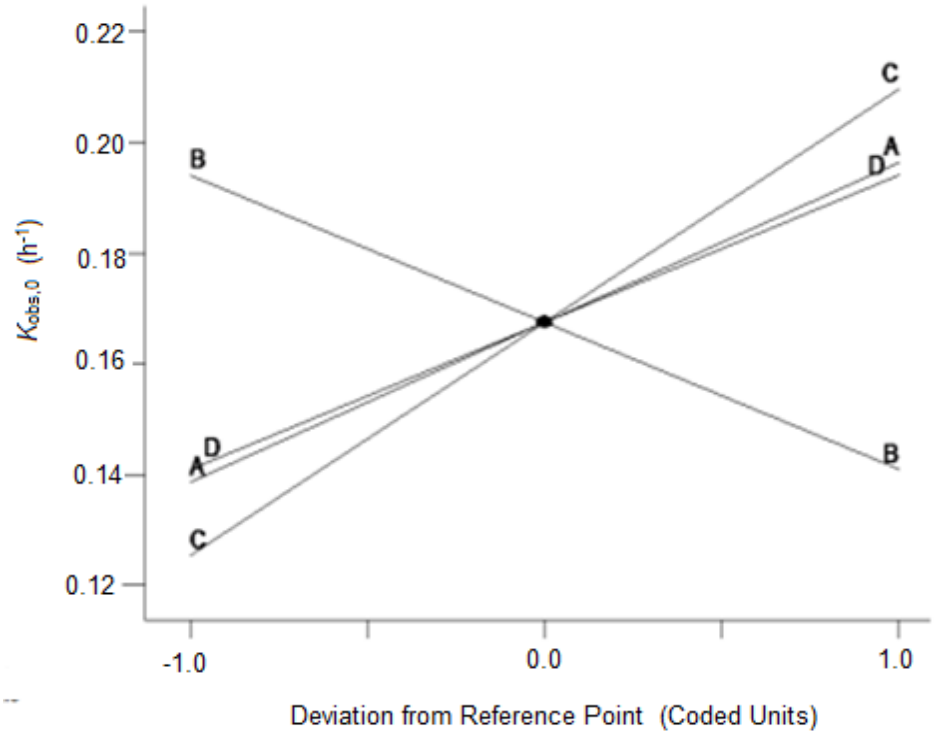

(b)

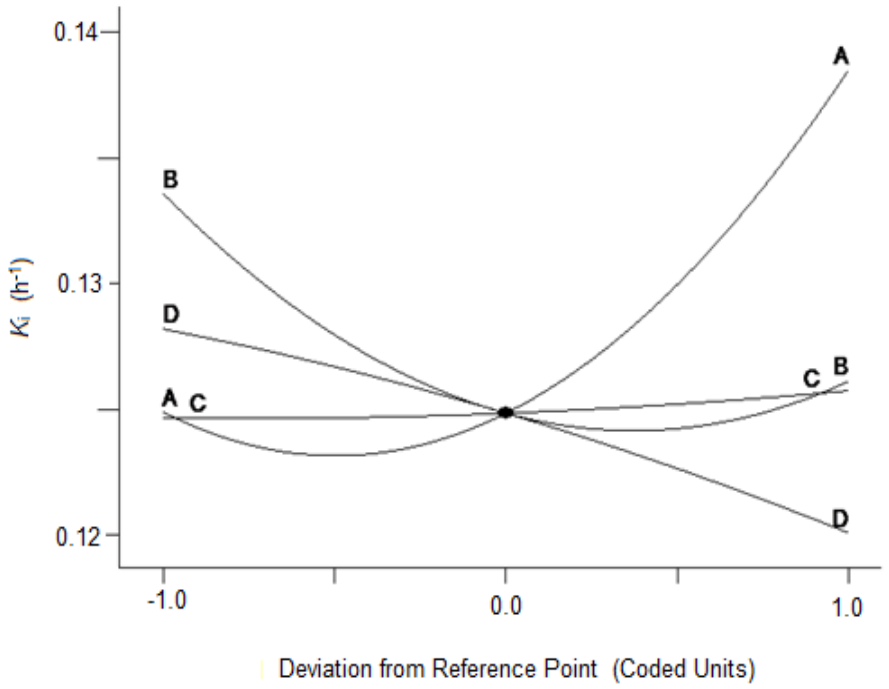

(c)

Fig. 2. Perturbation of the response surface methods; (a) Y_{trs}, (b) $K_{obs,0}$, and (c) K_i

In conclusion, the optimal medium for maximum Y_{trs} was determined using a one-factor-at-a-time design and a BBD-RSM. The predicted maximum Y_{trs}, $K_{obs,0}$, and minimum K_i were 55.56%, 0.3656 h^{-1}, and 0.1100 h^{-1}, respectively. The predicted value of Y_{trs} was relatively high compared to previously reported yields (Zhang *et al*. 2015; Chakraborty *et al*. 2016). The optimized conditions were a pH of 4.7, a temperature of 48.6 °C, a cellulase concentration of 1.5%, and a water to materials ratio of 12.4. Using the optimized culture medium, 2 kg of CS pretreated with H_2O_2 and LiP-containing *A. oryzae* CGMCC 5992 broth was hydrolyzed. The Y_{trs}, $K_{obs,0}$, and K_i reached 58.28%, 0.3532 h^{-1}, and 0.1323 h^{-1}, respectively, after 12 h of hydrolysis, which was consistent with the results of RSM optimization.

Analysis of Correlation Between Y_{trs}, $K_{obs,0}$, and K_i

The Impeded Michaelis model was developed and verified, indicating that it could be applied to other hydrolysis systems (Yang and Fang 2015a,b). The *p* values were less than 0.01 and R^2 was higher than 0.9 in all regression equations in the above-described experiments, which suggested that the Impeded Michaelis model fit the results well. By providing $K_{obs,0}$ and $K_{i,}$, the model helped to illustrate the mechanism through which each condition affected Y_{trs} in the process of lignocellulose saccharification. However, the model was not able to show the correlation between Y_{trs} and $K_{obs,0}$ or K_i, which was a disadvantage.

Because $K_{obs,0}$ was equal to $k_2[E_0]$ / K_m, and $[E_0]$ was the initial cellulase concentration, which was a constant, $K_{obs,0}$ was proportional to k_2 / K_m. The variable k_2 represents the rate constant facilitating reactions from enzymatic-substrate complex to final products. The greater the value of k_2, the higher the final product (reducing sugar) concentration will be (Y_{trs}). The term K_m represents the Michaelis-Menten constant, which reflects the concentration of the substrate when the reaction velocity is equal to one half of the maximal velocity for the reaction. The smaller the value of K_m, the greater the affinity, the greater the value of Y_{trs} and *vice versa.* Therefore, it was reasonable to deduce that Y_{trs} was positively correlated with $K_{obs,0}$. The variable K_i is the coefficient of ineffective enzyme during the hydrolysis reaction, thus a lower value of K_i indicated less ineffective enzyme and more effective enzyme. Taken together, the authors believed that the Y_{trs} was negatively correlated with K_i.

To verify the two deductions, the authors analyzed the data on Y_{trs}, $K_{obs,0}$, and K_i in Tables 2, 3, 5, and 6 with a more simple and intuitive binary quadratic regression using the following function,

$$Y_{trs} = \alpha \times (K_{obs,0})^2 + b \times K_{obs,0} - c \times (K_i)^2 + d \times K_i - 139 \quad (10)$$

where α, b, c, and d are the coefficients of $(K_{obs,0})^2$, $K_{obs,0}$, $(K_i)^2$, and K_i, respectively, and e is a constant.

Table 8. Coefficient of Regression Analysis of Items between Y_{trs}, $K_{obs,0,}$ and K_i*

Item	Coefficient	Standard Error	*t*-value	p value *
Constant	-139.270	31.498	-4.422	0.000
($K_{obs,0}$)2	-306.0110	11.054	26.268	0.000
$K_{obs,0}$	290.1671	491.986	6.156	0.000
(K_i)2	-15131.1670-	24.203	-12.655	0.000
K_i	3028.2850	1905.359	-7.941	0.000

*: F-value = 574.458, p = 0.000, R^2 = 0.9801, adj-R^2 = 0.9779

Table 8 shows the variance analysis of the relationships among Y_{trs}, $K_{obs,0}$, and K_i. From Table 8, the F value of the Fisher's test (574.458) and the *p* value of the t-test (0.000) showed that the correlation among Y_{trs}, $K_{obs,0}$, and K_i was extremely significant, and that the credibility of the analysis was extremely high. The fitness of the model was also confirmed by the R^2 value. The value for R^2 was 0.9801, which was higher than the reported highest R^2 value of 0.80 in a good fitting model (Govarthanan *et al*. 2015). This indicated that the predictability of the present model was relatively more reliable and that only 2% of the total variations were unable to be explained by the model. The adjusted R^2 was 0.9779, which was very close to the R^2 value. The proximity of the adjusted R^2 to R^2 suggested a good fitness of the model. The column diagram of model with better gaussian distribution could further establish the goodness of fit of the developed model Fig. 3. The analysis in Table 8 demonstrated that a significant correlation existed among Y_{trs}, $K_{obs,0}$, and K_i.

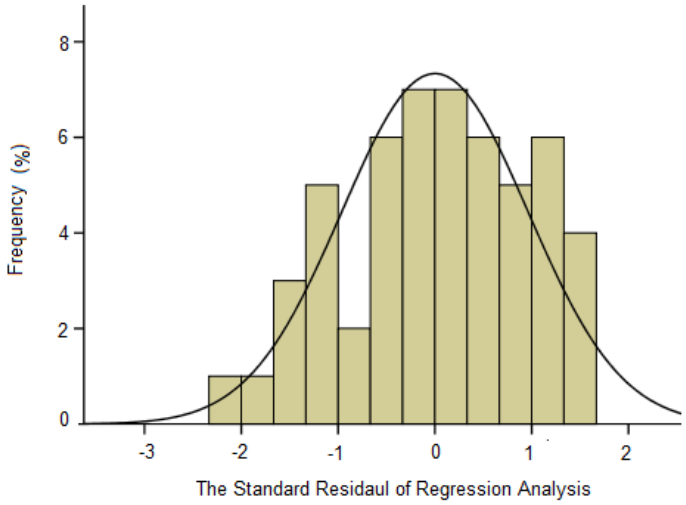

Fig. 3. The column diagram of the standard residual of regression analysis; the dependent variable: Y_{trs}; the independent variables: $K_{obs,0}$ and K_i; the standard error = 0.961; and *df* = 54

Coefficients for all of the parameters were extremely significant (p = 0.000). The negative coefficients of $(K_{obs,0})^2$ and $(K_i)^2$ in Table 8 demonstrated that the relationship curve between Y_{trs} and $K_{obs,0}$ or between Y_{trs} and K_i appeared to have an inverted-U-shaped relationship, and that Y_{trs} had the maximum value. After the coefficient of each item in Table 8 was introduced into Eq. 10, the equation below was given.

$$Y_{trs} = -306 \times (K_{obs,0})^2 + 290 \times K_{obs,0} - 15131 \times (K_i)^2 + 3028 \times K_i - 139 \quad (11)$$

The following two equations were obtained by taking the derivation of p_t to $K_{obs,0}$ and K_i, respectively.

$$Y_{trs}' = -612 \times K_{obs,0} + 290 \quad (12)$$

$$Y_{trs}' = -30262 \times K_i + 3028 \quad (13)$$

Suppose that Y_{trs}'= 0, $K_{obs,0}$ = 290 / 612 = 0.4739, and K_i = 3028 / 30262 = 0.1001. When $K_{obs,0}$ < 0.4739 and K_i < 0.1001, it follows that Y_{trs}' > 0, which could have been explained by the finding that Y_{trs} was significantly positively correlated with $K_{obs,0}$ and K_i. Conversely, when $K_{obs,0}$ > 0.4739 and K_i > 0.1001, then Y_{trs}' < 0, which could have been explained by the finding that Y_{trs} was significantly negatively correlated with $K_{obs,0}$ and K_i. When $K_{obs,0}$ = 0.4739 and K_i = 0.1001, Y_{trs} reached its maximum (82.07%). In Table 3 and Table 6, all $K_{obs,0}$ values were less than 0.4739 and all K_i values were higher than 0.1001. The Y_{trs} was positively correlated with $K_{obs,0}$ and negatively correlated with K_i. Because $K_{obs,0}$ was the initial activity and accessibility of enzyme on the substrate and K_i was the coefficient of ineffective enzyme during the hydrolysis reaction, the Y_{trs} was positively correlated with the initial activity and accessibility of the enzyme on the substrate and negatively correlated with the coefficient of ineffective enzyme during the hydrolysis reaction. The regression analysis could more simply and intuitively exhibit the correlation between Y_{trs} and $K_{obs,0}$ and the correlation between Y_{trs} and K_i than the Impeded Michaelis model.

CONCLUSIONS

1. A simplified Impeded Michaelis kinetic model containing two independent variables ($K_{obs,0}$ and a) and one dependent variable (Y_{trs}) could be applied to fit the data of the saccharification reaction cellulose of CS after pre-treatment with a combination of LiP and H_2O_2. The K_i was calculated from the variable a.
2. One-factor-at-a-time experimentation and RSM were applied to optimize the conditions for obtaining maximum Y_{trs} and $K_{obs,0}$ and minimum K_i. After optimization, the maximum Y_{trs} (55.56%) was obtained.
3. The binary quadratic function model fit the correlations between Y_{trs} and $K_{obs,0}$ and between Y_{trs} and K_i. The profile curves between Y_{trs} and $K_{obs,0}$ and between Y_{trs} and K_i presented an inverted-U-shaped curve.
4. Under the tested conditions, Y_{trs} was significantly and positively correlated with $K_{obs,0}$ and negatively correlated with K_i.

ACKNOWLEDGEMENTS

The authors would like to sincerely thank the following for their generous research grant funding: Taixing Yiming Bioproduction Co. Ltd., the Scientific and Technological Innovation Projects of Jiangsu Province General University Graduate Students (No. CXLX13687), the National Natural Science Foundation of China (No.31101269), the China Postdoctoral Science Foundation (2015M571691), the Senior Talent Scientific Research Initial Funding Project of Jiangsu University (15JDG061), and the 2014 Excellent Key Young Teachers Project of Jiangsu University.

REFERENCES CITED

Amini, M., Younesi, H., and Bahramifar, N. (2009a). "Statistical modeling and optimization of the cadmium biosorption process in an aqueous solution using *Aspergillus niger*," *Colloids Surf. A- Physicochem. Eng. Asp.* 337(1-3), 67-73. DOI: 10.1016/j.colsurfa.2008.11.053

Amini, M., Younesi, H., and Bahramifar, N. (2009b). "Biosorption of nickel (II) from aqueous solution by *Aspergillus niger*: Response surface methodology and isotherm study," *Chemosphere* 75(11), 1483-1491. DOI: 10.1016/j.chemosphere.2009.02.025

Balat, M.., and Balat, H. (2008). "Progress in bioethanol processing," *Prog. Energy Combust. Sci.* 34(5), 551-573. DOI: 10.1016/j.pecs.2007.11.001

Bansal, P., Hall, M., Realff, M. J., Lee, J. H., and Bommarius, A. S. (2009). "Modeling cellulase kineticson lignocellulosic substrates," *Biotechnol. Adv.* 27(6), 833-848. DOI: 10.1016/j.biotechadv.2009.06.005

Baeyens, J., Kang, Q., Appels, L., Dewil, R., Lv, Y., and Tan, T. (2015). "Challenges and opportunities in improving the production of bio-ethanol," *Prog. Energy Combust. Sci*. 47(1), 60-88. DOI:10.1016/j.pecs.2014.10.003

Beg, Q. K., Sahai, V., and Gupta, R. (2003). "Statistical media optimization and alkaline protease production from *Bacillus mojavensis* in a bioreactor," *Process Biochem.* 39(3), 203-209. DOI: 10.1016/S0032-9592(03)00064-5

Bellido, C., Loureiro-Pinto, M., Coca, M., Gonzalez-Benito, G., and Garcia-Cubero, M. T. (2014). "Acetone-butanol-ethanol (ABE) production by *Clostridium beijerinckii* from wheat straw hydrolysates: Efficient use of penta and hexa carbohydrates," *Bioresource Technol.* 167(1), 198-205. DOI: 10.1016/j.biortech.2014.06.020

Biswas, R., Teller, P. J., and Ahring, B. K. (2015). "Pretreatment of forest residues of douglas fir by wet explosion for enhanced enzymatic saccharification," *Bioresource Technol.* 192(1), 46-53. DOI: 10.1016/j.biortech.2015.05.043

Biswas, R., Uellendahl, H., and Ahring, B. K. (2015). "Wet explosion: A universal and efficient pretreatment process for lignocellulosic biorefineries," *Bioenerg. Res.* 8(3), 1101-1116. DOI: 10.1007/s12155-015-9590-5

Cao, W., Sun, C., Qiu, J., Li, X. D., Liu, R. H., and Zhang, L. (2016). "Pretreatment of sweet sorghum bagasse by alkaline hydrogen peroxide for enhancing ethanol production," *Korean J. Chem. Eng.* 33(3), 873-879. DOI: 10.1007/s11814-015-0217-5

Cerino-Córdova, F. J., García-León, A. M., Garcia-Reyes, R. B., Garza-González, M. T., Soto-Regalado, E., Sánchez-González, M. N., and Quezada-López, I. (2011).

"Response surface methodology for lead biosorption on *Aspergillus terreus*," *Int. J. Environ. Sci. Technol.* 8(4), 695-704. DOI: 10.1007/BF03326254

Cerino-Córdova, F. J., García-León, A. M., Soto-Regalado, E., Sánchez-González, M. N., Lozano-Ramírezb, T., García-Avalos, B. C., and Loredo-Medrano, J. A. (2012). "Experimental design for the optimization of copper biosorption from aqueous solution by *Aspergillus terreus*," *J. Environ. Manag.* 95, S77-S82. DOI: 10.1016/j.jenvman.2011.01.004

Chakraborty, S., Gupta, R., Jain, K. K., and Kuhad, R. C. (2016). "Cost-effective production of cellulose hydrolysing enzymes from *Trichoderma sp*. RCK65 under SSF and its evaluation in saccharification of cellulosic substrates," *Bioprocess Biosyst. Eng.* 39(11), 1659-1670. DOI: 10.1007/s00449-016-1641-6

Dávila-Guzmana, N. E., Cerino-Córdova, F. J., Diaz-Floresb, P. E., Rangel-Mendez, J. R., Sánchez-González, M. N., and Soto-Regalado, E. (2012). "Equilibrium and kinetic studies of ferulic acid adsorption by Amberlite XAD-16," *Chem. Eng. J.* 183(1), 112-116. DOI: 10.1016/j.cej.2011.12.037

Gan, Q., Allen, S. J., and Taylor, G. (2003). "Kinetic dynamics in heterogeneous enzymatic hydrolysis of cellulose: An overview, an experimental study and mathematical modeling," *Process Biochem.* 38(7), 1003-1018. DOI: 10.1016/s0032-9592(02)00220-0

Govarthanan, M., Selvankumar, T., Selvam, K., Sudhakar, C., Aroulmoji, V., and Kamala-Kannan, S. (2015). "Response surface methodology based optimization of keratinase production from alkali-treated feather waste and horn waste using *Bacillus sp*. MG-MASC-BT," *J. Ind. Eng. Chem.* 27(6), 25-30. DOI: 10.1099/00207713-50-2-831

Guan, G. Q., Zhang, Z. C., Ding, H. X., Li, M., and Shi, D. F. (2015). "Enhanced degradation of lignin in corn stalk by combined method of *Aspergillus oryzae* solid state fermentation and H_2O_2 treatment," *Biomass. Bioenerg.* 81(2), 224-233. DOI: 10.1016/j.biombioe.2015.07.008

Guo, D. Z., Zhang, Z. C., Liu, D., and Chen, K. P. (2013). "A comparative study on the degradation of gallic acid (GA) by *Aspergillue oryzae* and *Phanerochaete chrysosporium*," *Water Sci. Technol.* 70(1), 175-181. DOI: 10.2166/wst.2014.213

Kang, Q., Huybrechts, j., Van Der Bruggen, B., Baeyens, J., Tan, T., and Dewil, R. (2014). "Hydrophilic membrances to replace molecular sieves in dewatering the bioethanol/water azeotropic mixture," *Sep. Purif. Technol.* 136(1), 144-149. DOI:10.1016/j.seppur.2014.09.009

Lan, T. Q., Lou, H., and Zhu, J. Y. (2012). "Enzymatic saccharification of lignocelluloses should be conducted at elevated pH 5.2–6.2," *Bioenerg. Res.* 6(2), 476-485. DOI: 10.1007/s12155-012-9273-4

Lee, D., Yu, A. H. C., and Saddle, J. N. (1994). "Evaluation of cellulase recycling strategies for the hydrolysis of lignocellulosic substrates," *Biotechnol. Bioeng*. 45(4), 328-436. DOI: 10.1002/bit.260450407

Liu, Y., Liu, T., Wang, X., Xu, L., and Yan, Y. (2011). "Biodiesel synthesis catalyzed by *Burkholderia cenocepacia* lipase supported on macroporous resin NKA in solvent-free and isooctane systems," *Energ. Fuel*. 25(9), 1206-1212. DOI: 10.1021/ef200066x

Liu, Y., Tan, H., Zhang, X., Yan, Y., and Hameed, B. H. (2010). "Effect of monohydric alcohols on enzymatic transesterification for biodiesel production," *Chem. Eng. J.* 157(2), 223-229. DOI: 10.1016/j.cej.2009.12.024

Miller, G. L. (1959). "Use of dinitrosalicylic acid reagent for determination of reducing sugars," *Anal. Chem*. 31(3), 426-428. DOI: 10.1021/ac60147a030

Mitchell, D. A., and Lonsane, B. K. (1993). "Definition, characteristics and potential," in: *Solid Substrate Cultivation*, H. W. Doelle, C. Rolz (eds.), Elsevier Applied Science, London, UK.

Movagharnejad, K., and Sohrabi, M. A. (2003). "A model for the rate of enzymatic hydrolysis of some cellulosic waste materials in heterogeneous solid–liquid systems," *Biochem. Eng. J*. 14(1), 1-8. DOI: 10.1016/S1369-703X(02)00104-3

Qing, Q., Zhou, L., Huang, M., Guo, Q., He, Y. C., Wang, L. Q., and Zhang, Y. (2016). "Improving enzymatic saccharification of bamboo shoot shell by alkalic salt pretreatment with H_2O_2," *Bioresource Technol*. 201(2), 230-236. DOI: 10.1016/j.biortech.2015.11.059

Ramadoss, G., and Muthukumar, K. (2015). "Influence of dual salt on the pretreatment of sugarcane bagasse with hydrogen peroxide for bioethanol production," *Chem. Eng. J.* 260(15), 178-187. DOI: 10.1016/j.cej.2014.08.006

Rosgaard, L., Andric, P., Dam-Johansen, K., Pedersen, S., and Meyer, A. S. (2007). "Effects of substrate loading on enzymatic hydrolysis and viscosity of pretreated barley straw," *Appl. Biochem. Biotech*. 143(1), 27-40. DOI: 10.1007/s12010-007-0028-1

Sasaki, M., Kabyemela, B., Malaluan, R., Hirose, S., Takeda, N., Adschiri, T., and Arai, K. (1998). "Cellulose hydrolysis in subcritical and supercritical water," *J. Supercrit. Fluid* 13(1), 261-268. DOI: 10.1016/S0896-8446(98)00060-6

Salum, T. F. C., Villeneuve, P., Barea, B., Yamamoto, C. I., Cóco, L. C., Mitchell, D. A., and Krieger, N. (2010). "Synthesis of biodiesel in column fixed-bed bioreactor using the fermented solid produced by *Burkholderia cepacia* LTEB11," *Process Biochem*. 45(8), 1348-1354. DOI: 10.1016/j.procbio.2010.05.004

Shi, J., Chinn, M. S., and Sharma-Shivappa, R. R. (2008). "Microbial pretreatment of cotton stalks by solid state cultivation of *Phanerochaete chrysosporium*," *Bioresource Technol*. 99(4), 6556-6564. DOI: 10.1016/j.biortech.2007.11.069

Sluiter, B., Hames, R., Ruiz, C., Scarlata, J., Sluiter, J., Templeton, D., and Crocker, D. (2008). "Laboratory analytical procedure (LAP): *Determination of Structural Carbohydrates and Lignin in Biomass* (Report NREL/TP-510-42618), National Renewable Energy Laboratory, Golden, Co, USA.

Tanyildizi, M. S., Özer, D., and Elibol, M. (2005). "Optimization of a-amylase production by *Bacillus sp*. using response surface methodology," *Process Biochem*. 40(7), 2291-2296. DOI: 10.1016/j.procbio.2004.06.018

Vallander, L., and Eriksson, K. E. (1987). "Enzyme recirculation in saccharification of lignocellulosic materials," *Enzyme Microb. Tech*. 9(12), 714-720.

Wang, W., Zhu, Y., Du, J., Yang, Y., and Jin, Y. (2015). "Influence of lignin addition on the enzymatic digestibility of pretreated lignocellulosic biomasses," *Bioresource Technol*. 181(1), 7-12. DOI: 10.1016/j.biortech.2015.01.026

Xu, F., and Ding, H. A. (2007). "A new kinetic model for heterogeneous (or spatially confined) enzymatic catalysis: contributions from the fractal and jamming (overcrowding) effects," *Appl. Catal. A- Gen*. 317(1), 70-81. DOI: 10.1016/j.apcata.2006.10.014

Yang, C. Y., and Fang, T. J. (2015a). "Kinetics for enzymatic hydrolysis of rice hulls by the ultrasonic pretreatment with a bio-based basic ionic liquid," *Biochem. Eng. J*. 100(1), 23-29. DOI: 10.1016/j.bej.2015.04.012

Yang, C. Y., and Fang, T. J. (2015b). "Kinetics of enzymatic hydrolysis of rice straw by the pretreatment with a bio-based basic ionic liquid under ultrasound," *Process Biochem*. 50(4), 623-629. DOI: 10.1016/j.procbio.2015.01.013

Ye, Z., and Berson, R. E. (2011). "Kinetic modeling of cellulose hydrolysis with first order inactivation of adsorbed cellulose," *Bioresource Technol*. 102(24), 11194–11199. DOI: 10.1016/j.biortech.2011.09.044

Zhang, Z, C., Jia, J., Li, M., and Pang, Q. X. (2014). "H_2O_2 can increase lignin disintegration and decrease cellulose decomposition in the process of solid-state fermentation (SSF) by *Aspergillus oryzae* using corn stalk as raw materials," *BioResources* 9(2), 3077-3087. DOI: 10.15376/biores.9.2.3077-3087

Zhang, Z., Xia, L., Wang, F., Lv, P., Zhu, M. X. Q., Li, J. H., and Chen, K. P. (2015). "Lignin peroxidase in corn stalk by combined method of H_2O_2 hydrolysis and *Aspergillus oryzae* CGMCC5992 liquid-state fermentation," *Biotechnol. Biofuels* 8(2), 183-193. DOI: 10.1186/s13068-015-0362-4

Zhang, Z. C., Liu, D., Feng, F., Li, J. S., Li, M., and Pang, Q. X., and Chen, K. P. (2013). "Optimization of the nutrition for biodegradation of vinasse by *Aspergillus oryzae* using response surface methodology," *Water Sci. Technol.* 67(4), 772-779. DOI: 10.2166/wst.2012.631

Article submitted: March 2, 2017; Peer review completed: June 5, 2017; Revisions accepted: June 8, 2017; Published: June 13, 2017.
DOI: 10.15376/biores.12.3.5462-5486